

Performance and perspectives of silicon detector telescopes

F. Amorini^{a,c}, G. Bottiglieri^{d,e}, L. Caponetto^b, G. Cardella^b, A. Di Pietro^a, G. Fallica^d, P. Figuera^a, E. Leonora^{b,c}, D. Lo Presti^{b,c}, A. Morea^d, M. Papa^b, G. Pappalardo^{a,c}, C. Petta^{b,c}, N. Randazzo^b, S. Reito^b, F. Rizzo^{a,c}, G.V. Russo^{b,c}, V. Sipala^{b,c}, G. Valvo^d.

^aINFN-Laboratori Nazionali del Sud, Via S. Sofia 44, I95123 Catania Italy

^bINFN-Sezione di Catania, I95123 Catania Italy

^cDipartimento di Fisica ed Astronomia, Università di Catania, I95123 Catania Italy

^dST-Microelectronics, Stradale Primosole 50, I95100 Catania Italy

^eEuropean School for Advances Study in Nuclear and Ionizing Radiation Technologies, Istituto Universitario di Studi Superiori, Università degli Studi di Pavia

A new concept of monolithic silicon telescope sensitive to the position is studied along with an integrated front-end electronics.

1. INTRODUCTION

The most restrictive requirement that nowadays nuclear physics asks to experimental apparatus is the capability to identify and characterize ions produced in nuclear reactions, performed both with stable and radioactive beams at low or intermediate energy.

In several experimental situations, these goals are achieved by means of detector telescopes through the ΔE -E technique. Here the simultaneous detection of energy loss and total energy by two devices gives access to the charge (and in the case of good resolution of the ΔE stage also mass) of the detected particle. The best choice in terms of easy handling, stability and low identification thresholds is offered by monolithic telescopes, where the ΔE and E stages are implemented on the same silicon wafer. Starting from the intuition of Kemmer [1], this idea was variously exploited along with the development of associated readout electronics [2-8].

The typical device developed by our collaboration is built starting from p^+ wells, realized with a boron low energy implantation followed by high temperature (1050 °C) diffusion up to 2 μm depth on an n^- bulk of 5000 $\Omega\text{ cm}$ resistivity; then a p^+ region acting as common ground electrode for two stages is obtained via high energy (~900 keV) boron implantation on the same bulk, and the electric contacts are created on both sides (e.g. [6]).

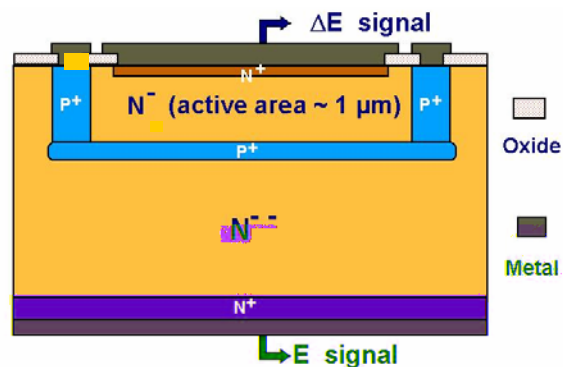


Fig. 1 Construction scheme (not in scale) of the implanted monolithic telescope.

The ultimate solution consists in a chip of 15x5 mm^2 , having 5 independent ΔE strips (3x4 mm^2 each) implanted on a common residual energy stage [7]. Two chips can be mounted in the same package to reduce the dead regions, see fig.2. The small area of each independent ΔE strip reduces the capacitance to about 1nF, allowing the use of commercial charge preamplifiers. The new ΔE -E telescopes have been produced in an industrial 6 inches wafer fab. The whole fabrication process is fully compatible with all the equipments used for other silicon devices. This is also due to the fact that

the wafers used for the new prototypes are 6" floating zone substrates with $\langle 1.0.0 \rangle$ crystal orientation.

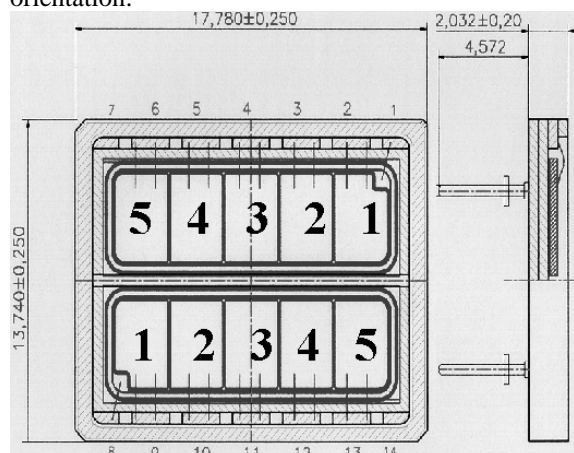


Fig. 2 Two detection chips assembling.

2. DETECTOR PERFORMANCES

The device was tested with a standard α source and under beam, and used in several experiments with different arrangements, together with other kind of detectors (e.g. gamma-rays detectors). As an example, fig. 3 shows a ΔE -E scatter plot coming from the collision $^{13}\text{N}+^9\text{Be}$ (induced by a radioactive ^{13}N beam) at 45 MeV incident energy. This spectrum shows a very good charge identification of the ions produced in the reaction.

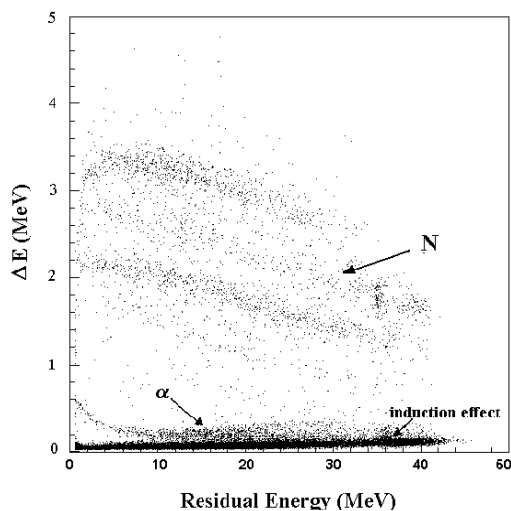


Fig. 3 ΔE versus residual energy spectrum measured in the collision $^{13}\text{N}+^9\text{Be}$ at 45 MeV.

The figure shows also a broad line corresponding to nearly zero ΔE signals. This “noise” comes from the fact that the charge created in the E stage without a physical signal in the ΔE (ions hitting other strips than the observed one or the dead zones of the detection unit) is collected in the common ground stage and induces a fast negative signal larger than the real positive one, as can be seen from the shape of the pulses shown in fig. 4. The origin of this phenomenon is the finite resistivity of the buried p^+ region.

Normally, the induction signal is a disturbing component of the signal and it is minimized by using large shaping times (3-6 μs) in the amplifier following the preamplifier [7]. On the contrary, by integrating the signal with a fast filter it is possible to study its behaviour in order to understand if it can be useful to enhance the global performances of the detector.

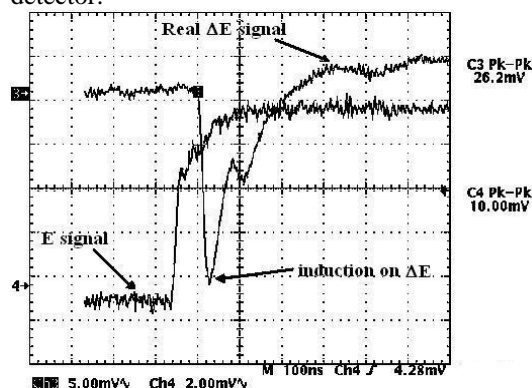


Fig. 4 Oscilloscope signals for one detector strip irradiated by an α source.

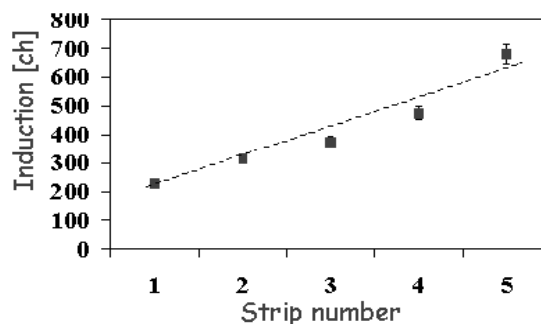


Fig. 5 Amplitude of the induction signal in strip 5 of the detector when trips from 1 to 5 ones are irradiated by an α source (see text).

To this purpose the detector was irradiated by a standard α source, and fig. 5 shows the amplitude of

the induction signal collected in strip 5 when a particle hits strips from 1 to 5 (see scheme in fig. 2).

These results showed a dependence of the induction from the position (strip) of the impinging particle, therefore a new device designed with the appropriate geometry could be also position sensitive.

3. SIMULATIONS AND ELECTRONICS DEVELOPMENT

To better understand the induction effect, simulations of the response of the monolithic device have been performed by means of the DESSIS code. These studies confirm the experimental evidence of the induced signal coming out from the ΔE stage together with the real one. The induction component results to be proportional to the energy loss in the E stage and its amplitude depends on the impact point of the particle on the detector. At the same time, a model was developed with a SPICE-like code, that gives the possibility to test easily several configurations and to optimise the design of the final readout.

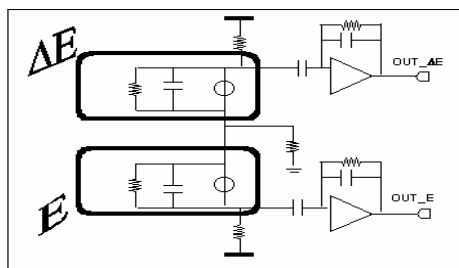


Fig. 6 Equivalent circuit for the monolithic detector and associated electronic chain.

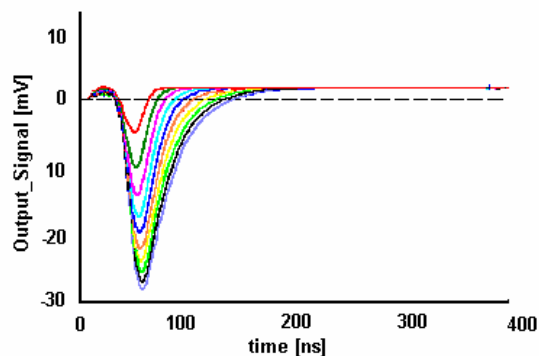


Fig. 7 Output signal of the CSA for the ΔE stage, simulated with SPICE-like model (see text for details).

Fig. 6 shows the equivalent circuit (detector and electronic chain) simulated and fig. 7 represents the obtained output of the Charge Sensitive Amplifier (CSA) connected to the ΔE stage. In these simulations we assumed a 5 MeV α particle, leaving 200 KeV on the first stage, and impinging in different points; from the strip closest to the ground contact (smallest amplitude curve) to the farthest one (larger amplitude). These curves were calculated with the SPICE-like model and are comparable to the DESSIS simulations. As it can be seen, the calculated shape of the pulse follows the effective behaviour of the observed one, showing the initial negative component and the following (slow) positive one. Moreover, these simulation are able to correlate the characteristics of the signal to the doping profiles and the topological properties of the buried layer. This turns out to be very useful for the design of the adequate electronic chain.

The amplitude of the induced signal for different impact points was simulated and it is represented in fig. 8, where a strong correlation is evident.

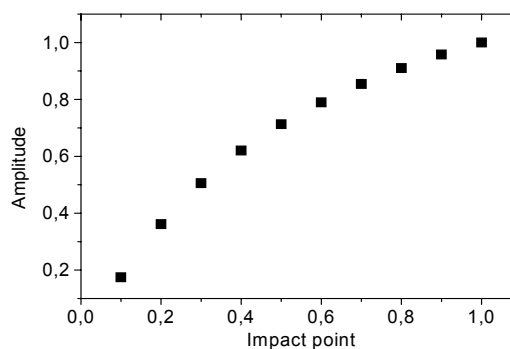


Fig. 8 Amplitude versus impact point of the induced signal on ΔE .

Starting from this information an integrated front-end electronics based on CMOS technology was designed. It is formed by a charge preamplifier followed by a semi-gaussian shaper. Special care will be devoted to the ΔE readout, due to its high capacitance.

The study of the noise performances, described in previous work [9,10], provides the best compromise for the signal output of the first stage. The results are shown in fig.9.

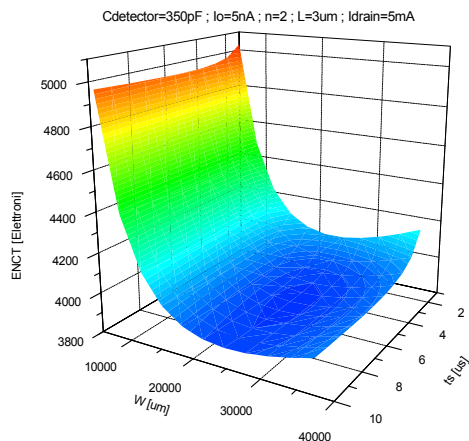


Fig. 9 Noise plot versus different design parameters (see text).

Fig. 9 shows a plot where the noise output is correlated to the characteristic parameters of the experimental setup, the detector and associated electronic chain. From a preliminary series of tests, a configuration where the noise problem is kept under acceptable values could be extracted, with the following specification:

Size = $400 \times 1000 \mu\text{m}^2$

Power supply = 5 V

Power dissipation < 15 mW

Noise @ 350 pF < 10 keV

Peaking time = 2-3 μs .

4. THE POSITION SENSITIVE DETECTOR

The results obtained from the experimental tests and the simulations revealed a strong dependence of the signal inducted on the first stage from the impact position of the impinging particle. Then we decided to design a new position sensitive monolithic telescope which is sketched in fig. 10.

As it can be seen, it will be constituted by independent ΔE strips that will provide the position information along the y axis, whereas the x coordinate will be extracted from the induction signal along the single strip. The best compromise between the global performances of the detector and the number and dimension of the strips was chosen on the basis of simulation discussed in the previous section. Then a first prototype will have 32 ΔE -strips, $15 \times 0.5 \text{ mm}^2$ each, implemented on a common E stage.

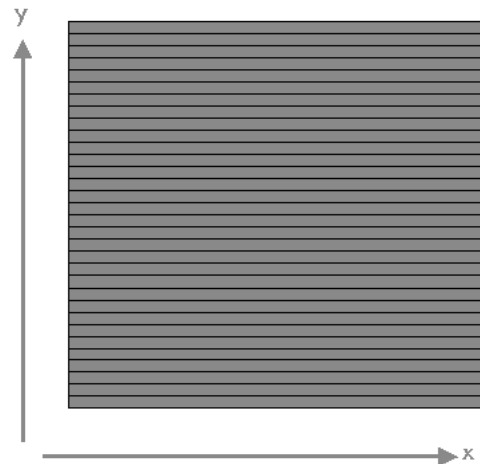


Fig. 10 Sketch of the new monolithic position sensitive telescope.

The potentialities of such kind of device will push its use beyond the field of pure nuclear physics experiments. In fact it could be used also for applied physics - for dosimetry and microdosimetry - to build devices to identify and monitor neutron flux, using appropriate converters for fast and slow neutrons.

REFERENCES

- [1] J. Kemmer, Diploma Thesis (2nd ed.), MPI Heidelberg, (1965)
- [2] C. Kim, H. Kim, K. Horiuchi, K. Husimi, S. Ohkawa, Y. Fuchi, IEEE Trans. Nucl. Science. 27 (1980) 258
- [3] Y. Kim Nucl. Instr. and Meth. 226 (1984) 125
- [4] J. von Borany et al., Nucl. Instr. and Meth. A377 (1996) 514
- [5] S. Thongstrom et al., Nucl. Instr. and Meth. **A391** (1997) 315
- [6] G. Cardella et al., Nucl. Instr. and Meth. A378 (1996) 262
- [7] A. Musumarra et al., Nucl. Instr. and Meth. A409 (1998) 414.
- [8] S. Tudisco et al., Nucl. Instr. and Meth. A426 (1999) 436.
- [9] N. Randazzo et al., IEEE Trans. Nucl. Sci. 44 (1997) 31.
- [10] N. Randazzo, et al., IEEE Trans. Nucl. Sci. 46 (1999) 1300.